Scientific Research Publishing

Journal of Applied Mathematics and Physics, 2020, 8, 2793-2800
https://www.scirp.org/journal/jamp
ISSN Online: 2327-4379
ISSN Print: 2327-4352

# A Micro-Sized Light-Driven Pico-Second Oscillator

**Ali J. Sabbah*, R. Hamam*#**

Math and Physics Department, Lebanese International University, Beirut, Lebanon
Email: #rafif.hamam@liu.edu.lb

**How to cite this paper:** Sabbah, A.J. and Hamam, R. (2020) A Micro-Sized Light-Driven Pico-Second Oscillator. *Journal of Applied Mathematics and Physics*, **8**, 2793-2800.
https://doi.org/10.4236/jamp.2020.812206

**Received:** October 1, 2020
**Accepted:** December 7, 2020
**Published:** December 10, 2020



## Abstract

Light carries linear momentum and can therefore exert a radiation force on the objects that it encounters. This established fact enabled optical manipulation of micro/nano-sized objects, as well as macroscopic objects such as solar sails, among many other important applications. While these efforts benefit from the average value of light's linear momentum, in this article, we propose exploiting the temporal variation of light's linear momentum to achieve an oscillatory force of microNewton amplitude and picosecond period. We validate our proposal by analytical calculations and time domain simulations of Maxwell's equations in the case of a high-index quarter-wave slab irradiated by a terahertz plane electromagnetic wave. In particular, we show that for plane wave terahertz light of electric field amplitude 5000 V/m and frequency 4.8 THz, an oscillatory radiation pressure of amplitude $1.8 \times 10^{-4}$ N/m$^2$ and 0.1 ps period can be achieved.

## Keywords

Radiation Force, Optical Manipulation/Micromachines, Instantaneous Electromagnetic Linear Momentum Density, Linear Momentum Conservation, Light Driven Oscillator

## 1. Introduction

Recent developments in micro and nano technologies have made it essential to devise elements suitable for nano/micro scale applications such as miniaturized machines that enable the manipulation of nano/micro sized objects [1] [2]. Various approaches have been developed ranging from optical [3] [4] [5] to opto-thermal [6], photophoretic [7], chemical [8] [9], nanofluidic [10], and even carbon nanotubes based approaches [11]. The majority of such efforts focus on

*Both authors contributed equally to this work.

optical tweezing, transport, and rotational manipulation, with fewer approaches addressing the vibrational control. The optical approaches to manipulate objects rely on the transfer of linear and/or angular momentum to matter [12] [13]. In particular, when light falls normally on a perfectly reflecting object, the average linear momentum that it carries pushes the object along light's propagation direction, and imparts it with an average linear momentum which is double that of incident light, due to the conservation of linear momentum involved in the reflection. However, for light of frequency $f$, the linear momentum density field $p$ also oscillates in time around a nonzero average value at a frequency $2f$. Although this oscillation in light's instantaneous linear momentum is too weak to produce macroscopic effects, we demonstrate theoretically, in this article how it may be exploited to produce oscillatory forces of μN amplitude that could be beneficial at the micro scale. While existing optical, opto-thermal, and photophoretic approaches to vibrational manipulation make use of inhomogeneous beams, such as strongly focused laser beams and helical light beams, our approach requires simply linearly polarized plane wave light.

## 2. Concept of Proposed Approach

We consider an $x$ polarized plane electromagnetic (EM) wave propagating along the $y$ direction in a medium of refractive index $n$, such that its electric field vector is described by:

$$\boldsymbol{E}(\boldsymbol{r},t)=\boldsymbol{i}E_o\sin\left(2\pi f\left(t-y/v\right)\right), \tag{1}$$

where $E_o$ is the electric field amplitude and $v\left(=c/n\right)$ is the speed of light in the medium. Such a wave carries a linear momentum density [14] [15]

$$\boldsymbol{p}=\boldsymbol{S}/v^2=\boldsymbol{E}\times\boldsymbol{B}/\left(\mu v^2\right), \tag{2}$$

where $\boldsymbol{S}$ is the Poynting vector, $\boldsymbol{B}$ is the magnetic field, and $\mu$ is the magnetic permeability (equal to the free space one $\mu_o=4\pi\times10^{-7}\,\mathrm{T\cdot m/A}$ since the medium is nonmagnetic). In particular, the $y$ component of the linear momentum density field is given by $p_y(\boldsymbol{r},t)=\left(n^2/\left(\mu_o c^2\right)\right)\left(-E_xB_z\right)$ since $E_z=0$. This linear momentum density component $p_y$ oscillates in time between 0 and $n^3E_o^2/\left(\mu_o c^3\right)$. Since $\boldsymbol{E}$ and $\boldsymbol{B}$ oscillate in time at light's frequency $f$, then $p_y\left(\sim E_xB_z\right)$ oscillates at double this frequency. Moreover, since light exchanges linear momentum with matter when it falls on it, then, it is possible to have matter's linear momentum acquire such an oscillatory behavior at a frequency $2f$. Such an oscillatory linear momentum also corresponds to an oscillatory force of frequency $2f$. For example, if one aims to have an oscillatory force of period 0.1 ps, then $f$ needs to be 4.835 THz, corresponding to a period $T=1/f=0.2$ ps, and a vacuum wavelength $\lambda$ of 62 μm, suitable for microscale applications.

## 3. Methods, Discussion and Results

We consider a quarter-wave slab of refractive index $n_{\mathrm{slab}}$ and thickness

$\Delta y = \lambda/(4n_{\text{slab}})$, which features significant reflection of incident light (and hence a significant transferred linear momentum) when $n_{\text{slab}}$ is high. For example, for GeTe, which has $n_{\text{slab}} = 7.3$ and $\kappa_{\text{slab}} = 0$ [16] [17], the quarter wave slab thickness is 2.1 μm for a terahertz light of wavelength 62 μm. Shorter wavelengths could be used if thinner slabs are desired, but in this case, the period of the oscillatory force will be shorter. The slab is taken to have a square cross section of dimension $w = 20\lambda = 1240\ \mu\text{m}$, and is surrounded by air regions above and below it. An $x$ polarized plane electromagnetic wave source, whose electric field is described by Equation (1) is turned on at $t = 0$ and is applied from a distance $10\lambda$ below the slab; this $10\lambda$ distance will enable us to observe the oscillatory force on the slab over a time interval of $10T$ after light reaches it. We therefore focus our attention on a computational domain whose two dimensional (2D) cross section is depicted in **Figure 1**, extending by $w = 20\lambda$ along $x$ and by $(20\lambda + \Delta y)$ along $y$.

In order to calculate the oscillatory force $F_y(t)$ on the slab, we perform two calculations for the $y$ component of light's linear momentum density field: once in the presence of the slab (we denote it by $p_{y,\text{light}}(\boldsymbol{r},t)$), and another time in the absence of the slab (we denote it by $p_{y,\text{light}}^{\text{Noslab}}(\boldsymbol{r},t)$). Then, in each calculation, we integrate the obtained linear momentum density field over the whole computational domain, and we obtain the $y$ components $P_{y,\text{light}}(t)$ and $P_{y,\text{light}}^{\text{Noslab}}(t)$ of light's total linear momentum in the presence of the slab and in its absence, respectively. From conservation of linear momentum, the $y$ component of the slab's linear momentum is

$$P_{y,\text{slab}}(t) = P_{y,\text{light}}^{\text{Noslab}}(t) - P_{y,\text{light}}(t), \tag{3}$$

and the oscillatory radiation force component $F_y(t)$ on the slab is $F_{y,\text{slab}}(t) = \mathrm{d}P_{y,\text{slab}}/\mathrm{d}t$.

Since it takes light a time of $10T$ (after source turn on) to reach the slab, it is evident that no radiation force acts on the slab in this time interval $0 \le t < 10T$. In this case, $p_{y,\text{light}}(\boldsymbol{r},t)$ is nonzero only for $y \le ct$, and as per Equation (2), is given by

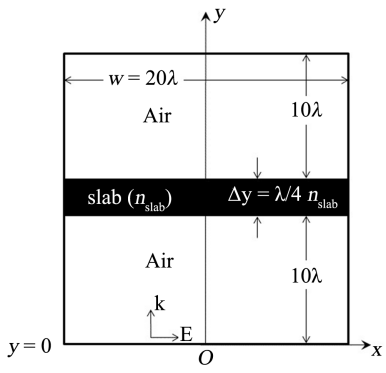


**Figure 1.** Schematic of the computational domain showing the quarter-wave slab surrounded by air. The incident wave is shown to propagate along $y$ with its $\boldsymbol{E}$ field polarized along the $x$ axis.

$$\begin{aligned} p_{y,\text{light}} &= \frac{E_o H_o}{c^2}\sin^2(\omega t - k_o y)\Theta(ct-y) \\ &= \frac{E_o H_o}{2c^2}\left[1-\cos(2k_o y - 2\omega t)\right]\Theta(ct-y), \end{aligned} \tag{4}$$

where $\omega = 2\pi f$ is the angular frequency, $k_o = 2\pi/\lambda$ is the free space angular wave number, $H_o = \frac{E_o n_{\text{air}}}{c\mu_o}$, and $\Theta(ct-y)$ is the step function (equal to 1 for $y < ct$ and zero otherwise). Integrating this expression for $p_{y,\text{light}}$ over the computational domain yields:

$$P_{y,\text{light}}^{\text{Noslab}}(t) = P_{y,\text{light}}(t) = \frac{E_o H_o w^2}{2c^2}\left[ct - \frac{\sin(2\omega t)}{2k_o}\right] \tag{5}$$

and $P_{y,\text{slab}}(t) = 0$.

After $10T$ from source turn on, the incident light, carrying an oscillatory linear momentum, starts to get continually reflected from the slab, and therefore, it keeps periodically imparting the slab with the same additional linear momentum every $T/2$. We therefore expect the slab to acquire an oscillatory linear momentum whose average value keeps building up and increasing linearly with time, which corresponds to an oscillatory radiation force of nonzero average value. To understand this behavior analytically, we obtain expressions for $p_{y,\text{light}}(\boldsymbol{r},t)$ and $p_{y,\text{light}}^{\text{Noslab}}(\boldsymbol{r},t)$ in the regions below, above, and inside the slab over the time interval $11T \le t \le 20T$. Since the main contribution to $P_{y,\text{slab}}(t)$ will be from the air regions above and below the slab, we may approximately write:

$$P_{y,\text{slab}}(t) \simeq w^2\left[\int_{y=0}^{10\lambda}\left(p_{y,\text{light}}^{\text{Noslab}} - p_{y,\text{light}}\right)\mathrm{d}y + \int_{y=10\lambda+\Delta y}^{20\lambda+\Delta y}\left(p_{y,\text{light}}^{\text{Noslab}} - p_{y,\text{light}}\right)\mathrm{d}y\right]. \tag{6}$$

In the air region below the slab ($0 \le y \le 10\lambda$), we have [18]:

$$p_{y,\text{light}}^{\text{Noslab}} = \frac{E_o H_o}{2c^2}\left[1-\cos(2k_o y - 2\omega t)\right], \tag{7}$$

and

$$\begin{aligned} p_{y,\text{light}} = \frac{E_o H_o}{2c^2}\Bigg\{&\left[1-\cos(2k_o y - 2\omega t)\right] \\ &-\left(\frac{2r}{1+r^2}\right)^2\left[1-\cos(2k_o y + 2\omega t)\right]\Theta(y - 20\lambda + ct)\Bigg\}, \end{aligned} \tag{8}$$

where $r = \frac{n_{\text{slab}} - n_{\text{air}}}{n_{\text{slab}} + n_{\text{air}}}$ is the amplitude reflection coefficient for the electric field ($r = 0.76$ for $n_{\text{slab}} = 7.3$), and the step function is used to take into consideration the fact that, at time $t$, there is no reflected light yet at $y < 20\lambda - ct$.

Similarly, in the air region above the slab ($10\lambda + \Delta y \le y \le 20\lambda + \Delta y$), we get:

$$p_{y,\text{light}}^{\text{Noslab}} = \frac{E_o H_o}{2c^2}\left[1-\cos(2k_o y - 2\omega t)\right]\Theta(ct-y), \tag{9}$$

and

$$p_{y,\text{light}} = \frac{E_o H_o}{2c^2}\left(\frac{1-r^2}{1+r^2}\right)^2 \left[1-\cos\left(2k_o y - 2\omega t\right)\right]\Theta\left(ct-y\right). \tag{10}$$

Substracting the above densities and then integrating over their corresponding regions gives the following approximate expression for $P_{y,\text{slab}}(t)$:

$$\begin{aligned} P_{y,\text{slab}}(t) \simeq \frac{E_o H_o w^2}{2c^2}&\left\{\left(\frac{2r}{1+r^2}\right)^2\left[ct-10\lambda-\frac{\sin\left(2\omega t\right)}{2k_o}\right]\right. \\ &\left.+\left[1-\left(\frac{1-r^2}{1+r^2}\right)^2\right]\left(ct-10\lambda-\Delta y\right)\right\} \\ &+\frac{E_o H_o w^2}{2c^2}\left[1-\left(\frac{1-r^2}{1+r^2}\right)^2\right]\frac{\sin\left(2k_o\Delta y-2\omega t\right)}{2k_o}, \end{aligned} \tag{11}$$

which is consistent with the expected oscillatory behavior for $P_{y,\text{slab}}(t)$ around a linearly increasing average value. Differentiating with respect to time yields an approximation for the oscillatory radiation force $P_{y,\text{slab}}(t)$ acting on the slab and having an average value

$$\left\langle F_{y,\text{slab}}\right\rangle = \frac{E_o H_o w^2}{2c^2}\left[\left(\frac{2r}{1+r^2}\right)^2+1-\left(\frac{1-r^2}{1+r^2}\right)^2\right]. \tag{12}$$

The corresponding average radiation pressure on the slab is $\left\langle F_{y,\text{slab}}\right\rangle / w^2$.

To validate the above analytical approximations, we performed numerical time domain simuations of Maxwell's equations based on the finite element method (locally available software) over the 2D computational domain depicted in Figure 2. Apart from the $y=0$ boundary where the source of Equation (1) is applied and turned on at $t=0$, radiation (second order absorbing) boundary condition [19] is used at the remaining domain boundaries. Given the $20\lambda\times\left(20\lambda+\Delta y\right)$ domain size, we limited the simulation time over the interval ranging from $t=0$ to $t=20T$, and we computed the electric and magnetic fields at each time step (step size $=0.05T$). The $y$ component $p_{y,\text{light}}$ of light's

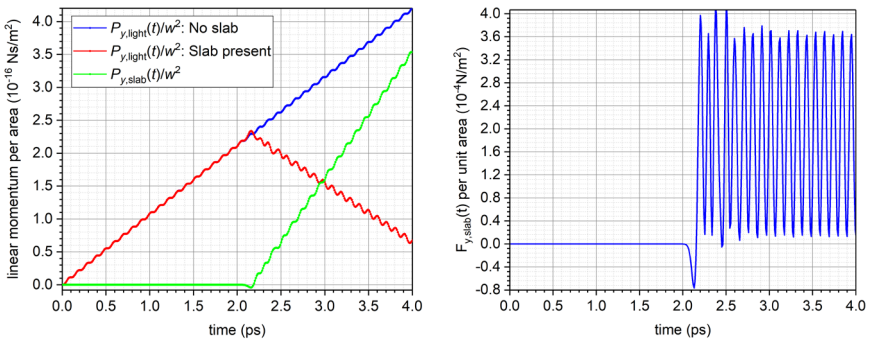


(a) (b)

Figure 2. (a) Plot showing the temporal dependence of the $y$ component of linear momentum (for light and for the slab) per unit cross sectional area $A=w^2$; (b) Plot of the $y$ component of the oscillatory force acting on the slab per unit area. Steady state oscillations are reached after around 3 ps.

linear momentum density field was then evaluated everywhere in the domain at each time step (by using Equation (2)), and then $p_{y,\text{light}}$ was integrated over the 2D computational domain at each time step to yield the $y$ component of light's linear momentum per unit depth along $z$, which, when multiplied by $w$, gives $P_{y,\text{light}}(t)$. The same simulation and procedure were then repeated with the slab being replaced by air, in order to obtain light's linear momentum component per unit $z$ length in the absence of the slab, which again, when multiplied by $w$, gives $P_{y,\text{light}}^{\text{Noslab}}(t)$. The slab's linear momentum was then computed by using Equation (3), and then differentiated to give the force component $F_y(t)$ on the slab.

In **Figure 2(a)**, we show the numerical results for the temporal dependence of light's linear momentum per unit cross sectional area ($A = w^2$) both in the presence and absence of the slab, in the case when $E_o = 5000\ \text{V/m}$. We also show how the slab's linear momentum per unit area varies with time. The results are consistent with the analytical expressions and the predicted behavior; soon after light reaches the slab, the slab's linear momentum acquires an oscillatory behavior with an average value that keeps building up linearly with time. In **Figure 2(b)**, we show, for the same parameters of **Figure 2(a)**, the oscillatory behavior for the radiation force per unit area (radiation pressure) acting on the slab. As expected, the force is oscillatory around a nonzero average value, and if one is interested in obtaining an oscillatory slab motion, then one needs to apply an external steady force equal and opposite to this average value, so as to keep only an oscillatory behavior for the radiation force around a zero average value, corresponding to a simple harmonic motion (SHM) of frequency $2f$. For $E_o = 5000\ \text{V/m}$, the amplitude of this oscillatory radiation force per unit area (radiation pressure) is $1.8 \times 10^{-4}\ \text{N/m}^2$, which for a slab of square cross section and dimension $w = 20\lambda$, corresponds to a force amplitude of 0.11 μN. This force amplitude can be adjusted by changing $E_o$, since it is proportional to $E_o^2$. Also, oscillations at other frequencies can be achieved by rescaling the slab's thickness.

## 4. Conclusion

In conclusion, we exploited the temporal variations of light's linear momentum together with conservation of linear momentum to propose a method of achieving an oscillatory force of μN amplitude and sub-picosecond period. We validated the proposed approach numerically by finite element simulations in which the instantaneous linear momentum density field is computed from the electric and magnetic fields at each time step, and is then integrated over space to obtain light's linear momentum at each moment of time. The proposed approach could be of relevance to medical applications and also to mechanical microdevices requiring terahertz mechanical oscillations.

## Conflicts of Interest

The authors declare no conflicts of interest regarding the publication of this paper.

## References


[1] Gao, D.L., Ding, W.Q., Nieto-Vesperinas, M., Ding, X.M., Mahdy, M.R.C., Zhang, T.H., Lim, C.T. and Qiu, C.-W. (2017) Optical Manipulation from the Microscale to the Nanoscale: Fundamentals, Advances, and Prospects. *Light*: *Science Applications*, **6**, e17039. https://doi.org/10.1038/lsa.2017.39

[2] Sierra, D., Weir, N. and Jones, J. (2005) A Review of Research in the Field of Nanorobotics. Sandia Report. https://doi.org/10.2172/875622

[3] Tong, L.M., Miljkovi, V.D. and Kll, M. (2010) Alignment, Rotation, and Spinning of Single Plasmonic Nanoparticles and Nanowires Using Polarization Dependent Optical Forces. *Nano Letters*, **10**, 268-273. https://doi.org/10.1021/nl9034434

[4] Neukirch, L.P. and Vamivakas, A.N. (2015) Nano-Optomechanics with Optically Levitated Nanoparticles. *Contemporary Physics*, **56**, 48-62.

[5] Li, M., Pernice, W., Xiong, C., Baehr-Jones, T., Hochberg, M. and Tang, H. (2008) Harnessing Optical Forces in Integrated Photonic Circuits. *Nature*, **456**, 480-484. https://doi.org/10.1038/nature07545

[6] Zhong, M.-C., Liu, A.-Y. and Ji, F. (2019) Opto-Thermal Oscillation and Trapping of Light Absorbing Particles. *Optics Express*, **27**, 29730-29737. https://doi.org/10.1364/OE.27.029730

[7] Shvedov, V., Davoyan, A., Gnatovsky, C., Engheta, N. and Krlikowski, W. (2014) A Long-Range Polarization-Controlled Optical Tractor Beam. *Nature Photonics*, **8**, 846-850. https://doi.org/10.1038/nphoton.2014.242

[8] Wang, B.Y. and Král, P. (2007) Chemically Tunable Nanoscale Propellers of Liquids. *Physical Review Letters*, **98**, Article ID: 266102. https://doi.org/10.1103/PhysRevLett.98.266102

[9] Zhang, Y., Calupitan, J.P., Rojas, T., Tumbleson, R., Erbland, G., Kammerer, C., Ajayi, T.M., Wang, S., Curtiss, L.A., Ngo, A.T., Ulloa, S.E., Rapenne, G. and Hla, S.W. (2019) A Chiral Molecular Propeller Designed for Unidirectional Rotations on A Surface. *Nature Communications*, **10**, Article No. 3742. https://doi.org/10.1038/s41467-019-11737-1

[10] Huh, D., Mills, K., Zhu, X.Y., Burns, M., Thouless, M. and Takayama, S. (2007) Tuneable Elastomeric Nanochannels for Nanofluidic Manipulation. *Nature Materials*, **6**, 424-428. https://doi.org/10.1038/nmat1907

[11] Lozovik, Yu.E., Minogin, A.V. and Popov, A.M. (2003) Nanomachines Based on Carbon Nanotubes. *Physics Letters A*, **313**, 112-121. https://doi.org/10.1016/S0375-9601(03)00649-2

[12] Shi, H. and Bhattacharya, M (2016) Optomechanics Based on Angular Momentum Exchange between Light and Matter. *Journal of Physics B*: *Atomic*, *Molecular and Optical Physics*, **49**, Article ID: 153001. https://doi.org/10.1088/0953-4075/49/15/153001

[13] Mansuripur, M. (2018) Energy, Linear Momentum, and Angular Momentum Exchange between an Electromagnetic Wave-Packet and a Small Particle. *Journal of Nanophotonics*, **13**, Article ID: 012503. https://doi.org/10.1117/1.JNP.13.012503

[14] Jackson, J.D. (1999) Classical Electrodynamics. Wiley, New York.

[15] Baxter, C. and Loudon, R. (2010) Radiation Pressure and the Photon Momentum in Dielectrics. *Journal of Modern Optics*, **57**, 830-842. https://doi.org/10.1080/09500340.2010.487948

[16] Okoye, C.M.I. (2002) Electronic and Optical Properties of SnTe and GeTe. *Journal of Physics*: *Condensed Matter*, **14**, 8625-8637.

https://doi.org/10.1088/0953-8984/14/36/318

[17] Baranov, D.G., Zuev, D.A., Lepeshov, S.I., Kotov, O.V., Krasnok, A.E., Evlyukhin, A.B. and Chichkov, B.N. (2017) All-Dielectric Nanophotonics: The Quest for Better Materials and Fabrication Techniques. *Optica*, **4**, 814-825. https://doi.org/10.1364/OPTICA.4.000814

[18] Hecht, E. (2002) Optics. Pearson Education, London.

[19] Bayliss, A. and Turkel, E. (1980) Radiation Boundary Conditions for Wave-Like Equations. *Communications on Pure and Applied Mathematics*, **33**, 707-725. https://doi.org/10.1002/cpa.3160330603